Computers and Geotechnics 95 (2018) 137–146

Contents lists available at ScienceDirect

Computers and Geotechnics

journal homepage: www.elsevier.com/locate/compgeo

Research Paper

Robust estimation of the fracture diameter distribution from the true trace length distribution in the Poisson-disc discrete fracture network model

Amin Hekmatnejad, Xavier Emery*, Javier A. Vallejos

Department of Mining Engineering, University of Chile, Avenida Tupper 2069, Santiago, Chile
Advanced Mining Technology Center, University of Chile, Avenida Beauchef 850, Santiago, Chile

ARTICLE INFO

Keywords:
Fracture network
Poisson-disc model
Fracture size
Distribution-free methods

ABSTRACT

A distribution-free approach is proposed to estimate the fracture size distribution from a given trace length distribution, assuming that the fracture network can be represented by a Poisson-disc model. This approach directly works on the experimental distribution of the observed trace lengths (corrected from sampling biases) and does not need to choose a parametric model for the trace length or fracture diameter distributions. It is more robust than existing models and provides an unbiased estimate of the cumulative distribution function of the fracture diameters. Its simplicity of use, accuracy and versatility are illustrated through synthetic examples.

1. Introduction

A comprehensive understanding of fracture networks is critical to the economic development of underground mining (cave ability, water drainage, roof stability, fragmentation, gas ventilation, flow gravity), open pit mining (slope stability, water drainage, blast ability, solution mining, in situ leaching), tailing dam (environmental aspects), oil and gas reservoir engineering (fractured reservoirs and unconventional reservoirs), generation of heat and vapor from geothermal reservoirs, management of groundwater resources and underground nuclear wastes disposal. The characterization of fracture networks is one of the most important parts of the engineering characterization of rock masses. The fracture properties that have the greatest influence at the design stage are location, orientation, size, frequency, surface geometry, genetic type and infill material [31,32].

One of the most interesting parameters of fracture networks is the fracture intensity, i.e. the mean area of fractures per unit volume [10]. A fixed fracture intensity can be the result of very different scenarios, such as a network of many small fractures or a network of few large fractures. As an example, for a given fracture intensity, there is a better connectivity with a few large fractures than with many small ones and, in terms of fragmentation, the size of blocks that are results of the intersections of the fracture network will change with different scenarios of the fracture sizes. Hence it is important to accurately estimate the distribution of fracture sizes.

To reach this objective, the available information usually consists of surface observations, namely trace lengths measured on exposures, such as natural outcrops, rock cuts and tunnel walls. One can distinguish three types of surface samplings: (1) scan line sampling that measures the trace lengths of the fractures that intersect a line drawn on the exposure; (2) circle sampling that measures the trace lengths of the fractures that intersect a circle drawn on the exposure; and (3) window or area sampling that measures the trace lengths of the fractures within a finite size area (such as a rectangle or a circular window) [3,11,8].

This paper focuses on the estimation of the fracture size distribution from the trace length distribution. It is outlined as follows. Section 2 presents the hypotheses and problem setting and a review of existing approaches for modeling the fracture size distribution knowing the trace length distribution. An alternative approach and its computational implementation are then introduced in Section 3. Numerical experiments on simulated fracture networks are presented in Section 4 to demonstrate the applicability, accuracy and robustness of the proposed approach. A general discussion and conclusions follow in Section 5.

2. State of the art

2.1. Modeling assumptions and problem statement

By setting up an object at each point of a 3D Poisson process, a Boolean model is obtained [27,28]. This object can be the same at every point or can be random, with a different shape, size and/or orientation. For fracture networks, the Boolean model often uses a circular disc as the object, which is known as the Poisson-disc model. This model has been first used for rock mechanics application by Baecher et al. [2]. The model parameters are the intensity of the Poisson point process, which

* Corresponding author at: Department of Mining Engineering, University of Chile, Avenida Tupper 2069, Santiago, Chile.
E-mail address: xemery@ing.uchile.cl (X. Emery).

http://dx.doi.org/10.1016/j.compgeo.2017.09.018
Received 25 April 2017; Received in revised form 23 August 2017; Accepted 27 September 2017
Available online 16 October 2017
0266-352X/

gives the average density of the points located in some region of space, and the joint distribution of the fracture orientations and fracture diameters. To enrich the model, other parameters such as fracture aperture and thickness could also be considered, which can be correlated with the fracture diameters [26,6], but will be out of the scope of this work.

The Poisson-disc model relies on the following assumptions:

(1) The fractures are modeled as two-dimensional circular discs scattered in the three-dimensional space, with random positions, diameters and orientations.
(2) The fracture diameters are independent and identically distributed (i.i.d.).
(3) The fracture orientations are independent and identically distributed. We do not assume any specific restriction on this distribution; in particular, the distributions of the fracture dips and dip directions can cover the full ranges of angles (0-90° for the dips and 0-360° for the dip directions) or any parts of these ranges.
(4) The fracture centers form a Poisson point process whose intensity is constant in space (homogeneous process).

These assumptions are basically the same as that used by Baecher et al. [2], Kulatilake and Wu [21], Zhang and Einstein [45], Song and Lee [40], Jimenez-Rodriguez and Sitar [18] and Song [38], among others. Using stereological considerations, Warburton [44] established the following relationship between the diameter distribution of the fractures with given orientation α (direction of the fracture pole, represented as a point of the 2-sphere S_2) and the distribution of their trace lengths on a given plane P:

$$f_\alpha^{(P)}(l) = \frac{l}{\mu_D(\alpha)} \int_l^{+\infty} \frac{g_\alpha(\delta)d\delta}{\sqrt{\delta^2-l^2}} \tag{1}$$

where $f_\alpha^{(P)}(l)$ is the probability density function (for short, *pdf*) of the trace lengths on plane P induced by the fractures with orientation α, while $\mu_D(\alpha)$ and $g_\alpha(\delta)$ are the expected value and the *pdf* of the diameters of such fractures with orientation α.

If one further assumes that the fracture diameter and fracture orientation are independent, then $g_\alpha(\delta)$ is actually independent of α and can be denoted as $g(\delta)$. Under this additional assumption, the *pdf* of the trace lengths induced by all the fractures on plane P is found by integrating Eq. (1) over all the possible orientations on the 2-sphere S_2, which gives

$$f(l) = \frac{l}{\mu_D} \int_l^{+\infty} \frac{g(\delta)d\delta}{\sqrt{\delta^2-l^2}} \tag{2}$$

where $f(l)$ is the *pdf* of the trace lengths on plane P induced by all the fractures, irrespective of their orientations, μ_D is the mean fracture diameter, and $g(\delta)$ is the *pdf* of the fracture diameters.

Note that the probability density function f does not depend on the particular plane P that has been chosen for observing the fracture trace lengths, as long as fracture diameters and fracture orientations are independent [42]. It corresponds to the *pdf* of the trace lengths observed on the whole plane P (equivalently, on a sampling window with an infinite size and with fixed and known orientation), which will be referred to as the "true" trace length *pdf*.

In practice however, trace lengths are measures in sampling windows with finite sizes and only a fraction of the fracture traces within the window may be measured. Accordingly, the measured trace length distribution usually differs from the true trace length distribution and suffers from orientation, size, truncation and censoring biases [3,11,33,21]. Several approaches have been proposed in the past decades to correct these sampling biases, which are out of the scope of this work (e.g., [44,33,30,25,21,43,29,34,40,46]).

In the following, the true trace length distribution (after correcting from sampling biases) will be supposed known. The problem is therefore to invert the integral in Eq. (2), in order to express the diameter probability density function (g) as a function of the true trace length probability density function (f).

Before proceeding, it is interesting to mention that the previous model assumptions can be weakened. First, the results further presented remain valid if the fracture diameters, fracture orientations and Poisson intensity are replaced by independent stationary ergodic random fields. Ergodicity guarantees that the experimental distributions observed over a large sampling domain are representative, up to statistical fluctuations, of the underlying model distributions, similarly to what happens with i.i.d. random variables [6,5]. The only requirement is thus to assume that the sampling window is large enough to observe the full distribution ranges of diameters, orientations and intensity. Note that randomizing the Poisson intensity converts the homogeneous Poisson process representing the fracture centers into a doubly stochastic Poisson process, also known as a Cox process.

Second, if the fracture diameters do not have an absolutely continuous distribution (e.g., if only a discrete set of fracture diameters are possible), one has to replace the numerator of the integrand in Eq. (2) ($g(\delta)d\delta$) by $dG(\delta)$, where $G(\delta)$ stands for the cumulative distribution function (*cdf*) of the fracture diameters. Up to this formal modification, all the equations and demonstrations presented hereafter remain valid. Note that, under the abovementioned assumptions for the Poisson-disc model, the trace length distribution is absolutely continuous and possesses a probability density function f that takes finite values except for the discontinuity points of G, as per Eq. (2), even if the density $g(\delta)$ takes infinite values for some specific values of δ or it is undefined (case of a non-absolutely continuous diameter distribution).

Third, if the fracture diameter and fracture orientation are not independent, Eq. (2) is no longer valid and one has to use Eq. (1) instead. One can therefore determine the diameter distribution of the fractures with a given orientation α (density g_α) by considering only the trace lengths on the sampling plane P induced by the fractures with orientation α (density $f_\alpha^{(P)}$), and repeat the procedure for different choices of the fracture orientation on the 2-sphere S_2. In practice, it is usual to distinguish a few fracture sets comprising approximately parallel fractures of the same type and age (for instance, fracture clusters whose distribution of orientations has a small dispersion). Based on Eq. (1), the formalism hereafter described can be applied to each fracture set separately.

2.2. Inverse and forward modeling

An inverse relationship for Eq. (2) is well-known in the fields of stereology and stochastic geometry [36,37,19,16]:

$$g(\delta) = -\frac{2\mu_D\delta}{\pi} \int_\delta^{+\infty} \frac{1}{\sqrt{l^2-\delta^2}} \frac{d}{dl}\left\{\frac{f(l)}{l}\right\} dl \tag{3}$$

This equation has been used by Tonon and Chen [41] to obtain the explicit expressions of the fracture diameter distribution for several commonly used trace length distributions (uniform, exponential, gamma and power law). For other trace length distributions such as the lognormal, the same authors propose a numerical approximation of Eq. (3). Other numerical methods have been suggested by Kulatilake and Wu [22], Song and Lee [40], Song [38], Song [39] and Zhu et al. [46], among others, to obtain the probability density function $g(\delta)$ of the fracture diameter distribution using the relationship between trace length and fracture diameter distributions (Eqs. (1) and (2) or equivalent stereological relationships). However, Eq. (3) involves the derivative of $f(l)/l$, the estimation of which lacks robustness in practice: a small variation of $f(l)$ may indeed produce a large variation of the derivative of $f(l)/l$, thus a large variation of $g(\delta)$, making the problem of

determining $g(\delta)$ from $f(l)$ an ill-posed problem [13].

To avoid this drawback, forward modeling techniques are often used instead, which consist in assuming a parametric density model for $g(\delta)$ (such as lognormal, negative exponential or gamma distributions) and determining the parameters, for instance by trial and error, so as to fit the distribution $f(l)$ of observed trace length data [43,24,9,45]. However, these forward techniques rely on choosing a family of fracture diameter distributions, so that different fits are obtained depending on the initial choice of this family of distributions. Also, the fitted distribution may not entirely agree with the experimentally observed trace length distribution, in particular, with its high-order moments.

In the following section, we propose an alternative approach for determining the cumulative distribution function of the fracture diameters (denoted as $G(\delta)$) instead of their probability density function $g(\delta)$. This approach avoids the definition of a given parametric model and results in a robust estimate of the fracture diameter distribution.

3. Proposed approach

3.1. Theoretical relationship between trace length and fracture diameter distributions

For $\delta \geq 0$, let us consider the following integral:

$$I(\delta) = \int_{\delta}^{+\infty} \frac{f(l)\,dl}{\sqrt{l^2-\delta^2}} \tag{4}$$

Accounting for Eq. (2), this integral can be expressed as follows:

$$I(\delta) = \frac{1}{\mu_D}\int_{\delta}^{+\infty}\left\{\int_{l}^{+\infty}\frac{g(D)dD}{\sqrt{D^2-l^2}}\right\}\frac{l\,dl}{\sqrt{l^2-\delta^2}} \tag{5}$$

Using Fubini's theorem, one obtains:

$$I(\delta) = \frac{1}{\mu_D}\int_{\delta}^{+\infty}\left\{\int_{\delta}^{D}\frac{l\,dl}{\sqrt{(D^2-l^2)(l^2-\delta^2)}}\right\}g(D)dD \tag{6}$$

Consider the change of variable $\cos^2(\theta) = \frac{D^2-l^2}{D^2-\delta^2}$ with $\theta \in [0,\frac{\pi}{2}]$. Then $\sin^2(\theta) = \frac{l^2-\delta^2}{D^2-\delta^2}$ and $-2\cos(\theta)\sin(\theta)d\theta = \frac{-2l\,dl}{D^2-\delta^2}$. Accordingly:

$$I(\delta) = \frac{1}{\mu_D}\int_{\delta}^{+\infty}\{\int_{0}^{\pi/2}d\theta\}g(D)dD = \frac{\pi}{2\mu_D}\int_{\delta}^{+\infty}g(D)dD \tag{7}$$

Let us denote by G the cumulative distribution function of the fracture diameters. From Eqs. (4) and (7), one obtains the following relationship between G and f:

$$1-G(\delta) = \frac{2\mu_D}{\pi}\int_{\delta}^{+\infty}\frac{f(l)\,dl}{\sqrt{l^2-\delta^2}} \tag{8}$$

For $\delta = 0$, one must have $G(0) = 0$, which entails that $f(l)/l$ must be integrable over $[0, +\infty[$. In particular, a necessary condition is that $f(0) = 0$: the density of true trace lengths must be zero for a zero length. This condition is sometimes (mistakenly) ignored when modeling the trace length distribution, e.g., when considering a uniform or an exponential distribution [35,4,2,7,17,33,20,1] (a justified example is given in Appendix A).

Under the assumption that $f(0) = 0$, one can integrate Eq. (8) by parts as follows:

$$\begin{aligned}1-G(\delta) &= \frac{2\mu_D}{\pi}\left[\frac{f(l)\sqrt{l^2-\delta^2}}{l}\right]_{\delta}^{+\infty} - \frac{2\mu_D}{\pi}\int_{\delta}^{+\infty}\frac{lf'(l)-f(l)}{l^2}\sqrt{l^2-\delta^2}\,dl \\ &= \frac{2\mu_D}{\pi}\int_{\delta}^{+\infty}\frac{f(l)-lf'(l)}{l^2}\sqrt{l^2-\delta^2}\,dl\end{aligned} \tag{9}$$

where $f'(l)$ is the derivative of the probability density function $f(l)$ of the true trace lengths. The probability density function $g(\delta)$ of the fracture diameters can be found by differentiation and application of Leibniz integral rule (derivation under the integral sign):

$$g(\delta) = \frac{2\mu_D\delta}{\pi}\int_{\delta}^{+\infty}\frac{f(l)-lf'(l)}{l^2\sqrt{l^2-\delta^2}}dl = -\frac{2\mu_D\delta}{\pi}\int_{\delta}^{+\infty}\frac{1}{\sqrt{l^2-\delta^2}}\frac{d}{dl}\left\{\frac{f(l)}{l}\right\}dl \tag{10}$$

This expression is the same as Eq. (3), which demonstrates that the approach we propose (Eq. (8)) is consistent with the existing modeling approaches. It is also worthy to note the similarity between this new approach and the one established by Emery et al. [12] in the field of mineral processing, when estimating the diameter distribution of air bubbles in a flotation cell.

3.2. Examples

To illustrate the proposed approach, let us assume that the fracture diameters have a beta distribution with shape parameters (a,b) and scale parameter D_{max}, i.e., their density g is:

$$g(D) = \begin{cases}\frac{\Gamma(a+b)}{D_{\max}\Gamma(a)\Gamma(b)}\left(\frac{D}{D_{\max}}\right)^{a-1}\left(1-\frac{D}{D_{\max}}\right)^{b-1} \text{ if } 0 < D < D_{\max} \\ 0 \text{ otherwise}\end{cases} \tag{11}$$

One can then calculate the density f of the trace lengths (Eq. (2)) by numerical integration. In turn, using the latter density, it is possible to re-calculate, by numerical integration, the complementary cumulative distribution function $1-G$ of the fracture diameters (Eq. (8)) and to compare it with the true complementary cumulative distribution function of the original beta distribution. When applied to three examples of beta distributions, the match between true and calculated distributions turns out to be perfect, up to machine precision error (Fig. 1).

3.3. Moments of the diameter distribution

For $p > 0$, define the moment of order p of the fracture diameter distribution as:

$$\mu_D^{(p)} = \int_0^{+\infty} D^p g(D)\,dD \tag{12}$$

Then, one has:

$$\begin{aligned}\mu_D^{(p)} &= \int_0^{+\infty}\left(\int_0^D p\,\delta^{p-1}d\delta\right)g(D)dD \\ &= \int_0^{+\infty}\left(\int_{\delta}^{+\infty}g(D)dD\right)p\,\delta^{p-1}d\delta \\ &= \int_0^{+\infty}[1-G(\delta)]\,p\,\delta^{p-1}d\delta\end{aligned} \tag{13}$$

Accounting for Eq. (8), this becomes:

$$\begin{aligned}\mu_D^{(p)} &= \frac{2p\mu_D}{\pi}\int_0^{+\infty}\left(\int_{\delta}^{+\infty}\frac{f(l)dl}{\sqrt{l^2-\delta^2}}\right)\delta^{p-1}d\delta \\ &= \frac{2p\mu_D}{\pi}\int_0^{+\infty}\left(\int_0^{l}\frac{\delta^{p-1}d\delta}{\sqrt{l^2-\delta^2}}\right)f(l)\,dl\end{aligned} \tag{14}$$

with $\int_0^l \frac{\delta^{p-1}d\delta}{\sqrt{l^2-\delta^2}} = l^{p-1}\int_0^1\frac{x^{p-1}dx}{\sqrt{1^2-x^2}} = l^{p-1}\frac{\sqrt{\pi}\,\Gamma(\frac{p}{2})}{2\Gamma(\frac{p+1}{2})}$ [14]. Accordingly, the moment of order p of the fracture diameter distribution, if it exists, is equal to

$$\mu_D^{(p)} = \frac{p\,\mu_D\,\Gamma\left(\frac{p}{2}\right)}{\sqrt{\pi}\,\Gamma(\frac{p+1}{2})}\mu_l^{(p-1)} \tag{15}$$

where $\mu_l^{(p-1)} = \int_0^{+\infty} l^{p-1}f(l)\,dl$ is the moment of order $p-1$ of the trace length distribution. This formula agrees with the one given by Zhang and Einstein [45] when p is an integer, but is actually valid for any positive real-valued p, which is a novel result with respect to the current literature. In particular, for $p = 2$ and $p = 3$, one obtains:

$$\mu_D^{(2)} = \frac{4\mu_D}{\pi}\mu_l^{(1)} \tag{16}$$

and

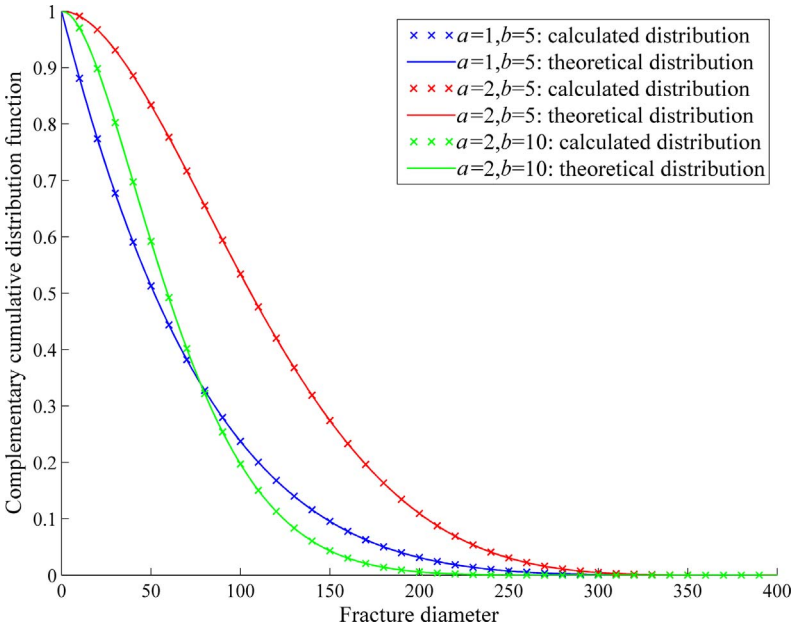

Fig. 1. True and estimated complementary cumulative distribution functions of fracture diameters. In all the cases, the scale parameter D_{max} is set to 400.

$$\mu_D^{(3)} = \frac{3\mu_D}{2}\mu_l^{(2)} \tag{17}$$

3.4. Computational implementation

In practice, the true trace length density f is approximated by a sample trace length density $\hat{f}$ that can be represented through the form of an histogram, i.e., $\hat{f}(l)$ is assumed constant over intervals $[\delta_i, \delta_{i+1}[$ with $i = 0,\ldots, n$ ($\delta_0 = 0$ and $\delta_{n+1} = +\infty$, while $\hat{f}(\delta_0) = \hat{f}(\delta_n) = 0$). In such a case, Eq. (8) can be approximated in the following fashion for $\delta = \delta_i$:

$$\begin{aligned} 1-G(\delta_i) &= \frac{2\mu_D}{\pi}\sum_{j=i}^{n}\int_{\delta_j}^{\delta_{j+1}}\frac{f(l)\,dl}{\sqrt{l^2-\delta_i^2}} \\ &\approx \frac{2\mu_D}{\pi}\sum_{j=i}^{n}\hat{f}(\delta_j)\int_{\delta_j}^{\delta_{j+1}}\frac{dl}{\sqrt{l^2-\delta_i^2}} \\ &= \frac{4\mu_D}{\pi}\sum_{j=i}^{n-1}\hat{f}(\delta_j)\ln\left(\frac{2\sqrt{\delta_{j+1}-\delta_i}+2\sqrt{\delta_{j+1}+\delta_i}}{2\sqrt{\delta_j-\delta_i}+2\sqrt{\delta_j+\delta_i}}\right) \end{aligned} \tag{18}$$

Because μ_D is unknown, it is actually more convenient to estimate $\varphi(\delta) = \frac{1-G(\delta)}{\mu_D}$:

$$\varphi(\delta_i) \approx \frac{4}{\pi}\sum_{j=i}^{n-1}\hat{f}(\delta_j)\ln\left(\frac{2\sqrt{\delta_{j+1}-\delta_i}+2\sqrt{\delta_{j+1}+\delta_i}}{2\sqrt{\delta_j-\delta_i}+2\sqrt{\delta_j+\delta_i}}\right) \tag{19}$$

For $i = 0$, one obtains

$$\varphi(0) = \frac{1}{\mu_D} \approx \frac{2}{\pi}\sum_{j=1}^{n-1}\hat{f}(\delta_j)\ln\left(\frac{\delta_{j+1}}{\delta_j}\right) \tag{20}$$

This formula allows estimating the mean diameter μ_D by putting $1/\varphi(0)$. Alternatively, if one considers that the distribution of fracture diameters is bounded by δ_i for some $i > 0$, one can also estimate μ_D as $1/\varphi(\delta_i)$, which may result in a more robust estimate than $1/\varphi(0)$ (see next section).

Once provided with an estimate of the mean diameter μ_D, Eq. (19) yields an estimation of the diameter cumulative distribution function $G(\delta) = 1 - \mu_D\,\varphi(\delta)$. Likewise, the moment of order p of the fracture diameter distribution can be estimated as follows (Eq. (15)):

$$\begin{aligned} \frac{\mu_D^{(p)}}{\mu_D} &= \frac{p\,\Gamma\left(\frac{p}{2}\right)}{\sqrt{\pi}\,\Gamma\left(\frac{p+1}{2}\right)}\int_0^{+\infty} l^{p-1}f(l)\,dl \\ &\approx \frac{\Gamma\left(\frac{p}{2}\right)}{\sqrt{\pi}\,\Gamma\left(\frac{p+1}{2}\right)}\sum_{i=0}^{n-1}\hat{f}(\delta_i)(\delta_{i+1}^p-\delta_i^p) \end{aligned} \tag{21}$$

4. Numerical experiments

4.1. Assumptions

In this section, we consider a fracture network consisting of a Poisson-disc model with a scaled beta distribution as the distribution of fracture diameters. Each of the experiments presented in the next subsections consists of the following steps:

(1) Choose an integer N (sample size).
(2) Choose an integer P (number of realizations or repetitions).
(3) Choose parameters for the fracture diameter distribution: D_{max} (maximum diameter), a and b (shape parameters) (Eq. (11)).
(4) Simulate a sample of N trace lengths. This is done by using an acceptance-rejection technique [23], based on the numerical calculation of the trace length density given in Eq. (2).
(5) Determine the histogram of the simulated trace lengths, which provides a discrete estimate of the probability density function $f(l)$. For practical calculations, unless for the third experiment, the range of possible trace length values (0 to D_{max}) is binned into regular intervals with a width of 1 unit.
(6) Apply the proposed approach (Eq. (19)) to determine $\varphi(\delta) = [1-G(\delta)]/\mu_D$.
(7) Repeat steps (4) to (6) P times in order to obtain P independent estimates of $\varphi(\delta)$ and compare these estimates with the true value of $\varphi(\delta)$, which can be calculated as the complementary cumulative distribution function of a beta distribution, properly rescaled.
(8) Estimate the mean fracture diameter μ_D as $1/\varphi(0)$ (option 1) or $1/\varphi(1)$ (option 2) and compare the estimates obtained over the P realizations with the true value.

Table 1
Parameters for first experiment.

Experiment	a	b	Maximum fracture diameter (D_{max})	Mean fracture diameter	Number of realizations (P)	Number of fracture traces (N)
1A	1	5	400	66.5	50	1000
1B	2	5	400	114.4	50	1000
1C	2	10	400	66.6	50	1000

The choice of the beta distribution at step (3) is motivated because this distribution takes on very different shapes on the interval in which it is defined, depending on its parameters. Other distributions could have been considered, although one should take care of the use of distributions that are not compactly supported (i.e., that differ from zero on an unbounded interval), such as the lognormal. Indeed, the associated trace length distribution would have the same property, which makes challenging the acceptance-rejection algorithm at step (4). In practice, such non-compactly supported diameter distributions have to be truncated to a sufficiently high maximum value, as shown in Appendix B, to implement the acceptance-rejection algorithm.

4.2. First experiment: Influence of the distribution shape

In the first experiment, three runs are performed with the same maximum fracture diameter ($D_{max} = 400$), same number of realizations ($P = 50$) and same sample size ($N = 1000$), but different shape parameters (a, b) for the distribution of fracture diameters (Table 1).

The estimates of φ(δ) are displayed in Fig. 2 (green curves), together with the results of the first realization (blue curve), the average estimate over the 50 realizations (red curve) and the true value of φ(δ) (black curve). One observes that, in all the cases, the estimated (green) curves fluctuate around the true (black) curve, and that their average (red curve) almost perfectly matches the true curve, which means that the estimator of φ(δ) proposed in Eq. (19) is unbiased.

Concerning the mean fracture diameter, its estimation by $1/\varphi(1)$ appears to be slightly more accurate, with a smaller average error over the 50 realizations, than by $1/\varphi(0)$ (Table 2). As the influence of diameters smaller than 1 over the mean value is marginal (due to their low probability of occurrence), the former estimator may be preferred to the latter.

4.3. Second experiment: Influence of the sample size

In the second experiment, we consider the fracture diameter distribution of experiment 1C (a beta distribution with shape parameters

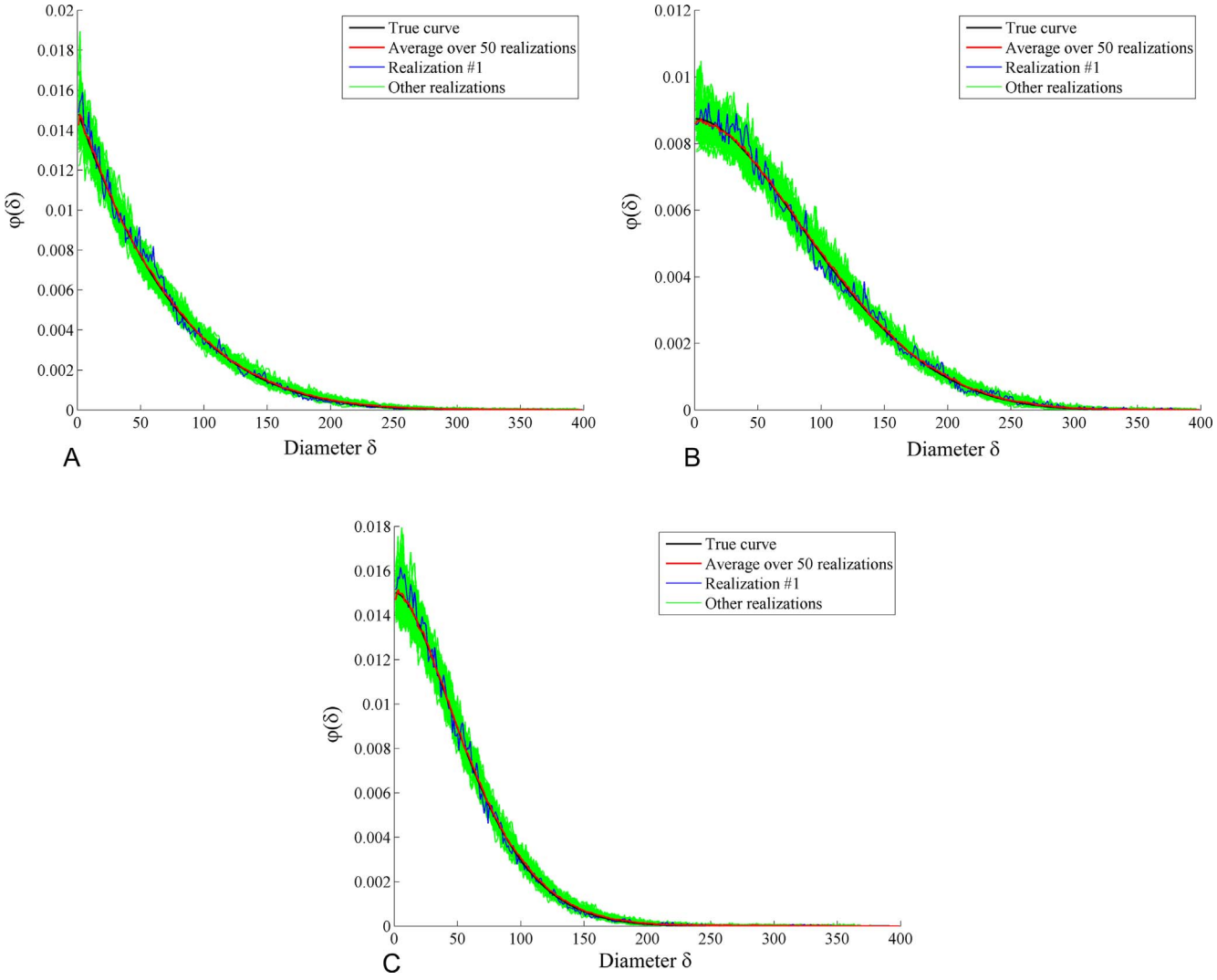

Fig. 2. Estimates of φ(δ) (blue and green), mean estimate (red) and true value (black) for experiments 1A, 1B and 1C.

Table 2
Estimates of mean diameter μ_D for first experiment.

Experiment	Estimator of μ_D	Minimum over P realizations	Maximum over P realizations	Average over P realizations	True value of μ_D
1A	$1/\varphi(0)$	59.7	81.9	70.4	66.5
1A	$1/\varphi(1)$	52.8	81.4	68.0	66.5
1B	$1/\varphi(0)$	106.2	128.8	116.7	114.4
1B	$1/\varphi(1)$	97.9	128.8	115.6	114.4
1C	$1/\varphi(0)$	61.8	73.2	68.2	66.6
1C	$1/\varphi(1)$	60.0	73.0	67.2	66.6

Table 3
Parameters for second experiment.

Experiment	a	b	Maximum fracture diameter (D_{max})	Mean fracture diameter	Number of realizations (P)	Number of fracture traces (N)
2A	2	10	400	66.6	50	100
2B	2	10	400	66.6	50	1000
2C	2	10	400	66.6	50	10,000

$a = 2$ and $b = 10$, rescaled between 0 and 400) and we modify the sample size, i.e., the number of observed fracture trace lengths, as stated in Table 3.

The estimates of $\varphi(\delta)$ still prove to be unbiased, insofar as the average over the realizations (red curve) is always close to the true (black) curve (Fig. 3). The fluctuations around the true curve decrease when the sample size increases, showing that the proposed estimator (Eq. (19)) is consistent, i.e., the estimation error tends to zero when the number of observed fracture trace lengths is very large.

Also, the fluctuations turn out to be more important for small diameters than for large ones and the estimate of $\varphi(0)$ is generally less robust (the red curve deviates more from the black curve at the origin)

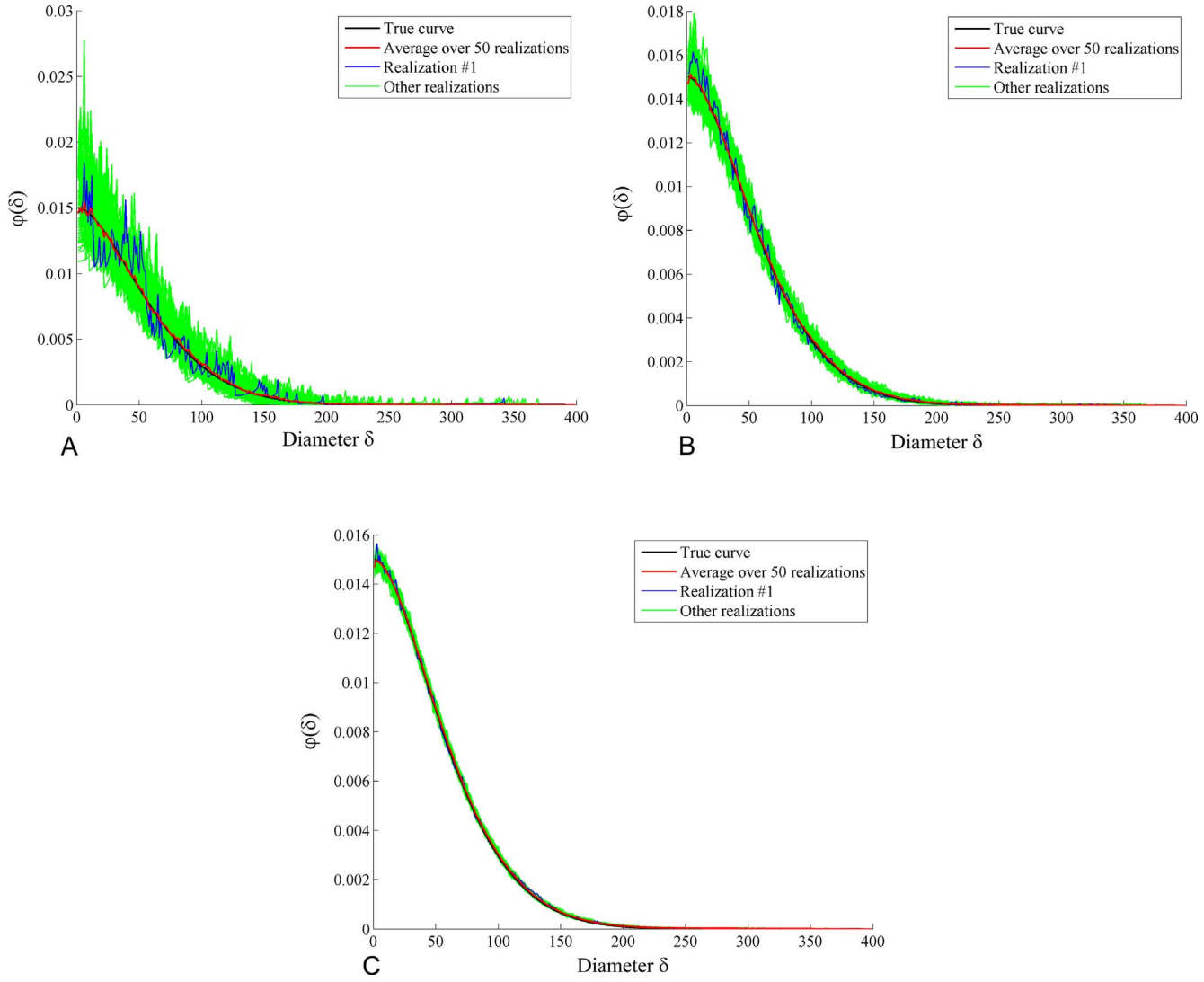

Fig. 3. Estimates of $\varphi(\delta)$ (blue and green), mean estimate (red) and true value (black) for experiments 2A, 2B and 2C.

Table 4
Estimates of mean diameter μ_D for second experiment.

Experiment	Estimator of μ_D	Minimum over P realizations	Maximum over P realizations	Average over P realizations	True value of μ_D
2A	$1/\varphi(0)$	53.0	91.5	69.6	66.6
2A	$1/\varphi(1)$	46.2	91.5	68.9	66.6
2B	$1/\varphi(0)$	61.8	73.2	68.2	66.6
2B	$1/\varphi(1)$	60.0	73.0	67.2	66.6
2C	$1/\varphi(0)$	66.4	70.0	68.1	66.6
2C	$1/\varphi(1)$	64.4	69.1	66.6	66.6

Table 5
Parameters for third experiment.

Experiment	a	b	Maximum fracture diameter (D_{max})	Mean fracture diameter	Number of realizations (P)	Number of fracture traces (N)	Binning class width for trace lengths
3A	2	10	400	66.6	50	1000	1
3B	2	10	400	66.6	50	1000	2
3C	2	10	400	66.6	50	1000	4
3D	2	10	400	66.6	50	1000	8

than that of $\varphi(1)$. This behavior is confirmed by the more accurate results obtained by estimating the mean diameter by $1/\varphi(1)$ rather than by $1/\varphi(0)$ (Table 4).

4.4. Third experiment: Influence of class binning

In the following experiment, we consider the same parameters as in experiment 1 C for the fracture diameter distribution ($a = 2$, $b = 10$, $D_{max} = 400$), number of realizations ($P = 50$) and sample size ($N = 1000$), but we modify the class width used for binning the histogram of simulated trace lengths, as specified in Table 5.

As observed in Fig. 4, the estimates of $\varphi(\delta)$ fluctuate around the true

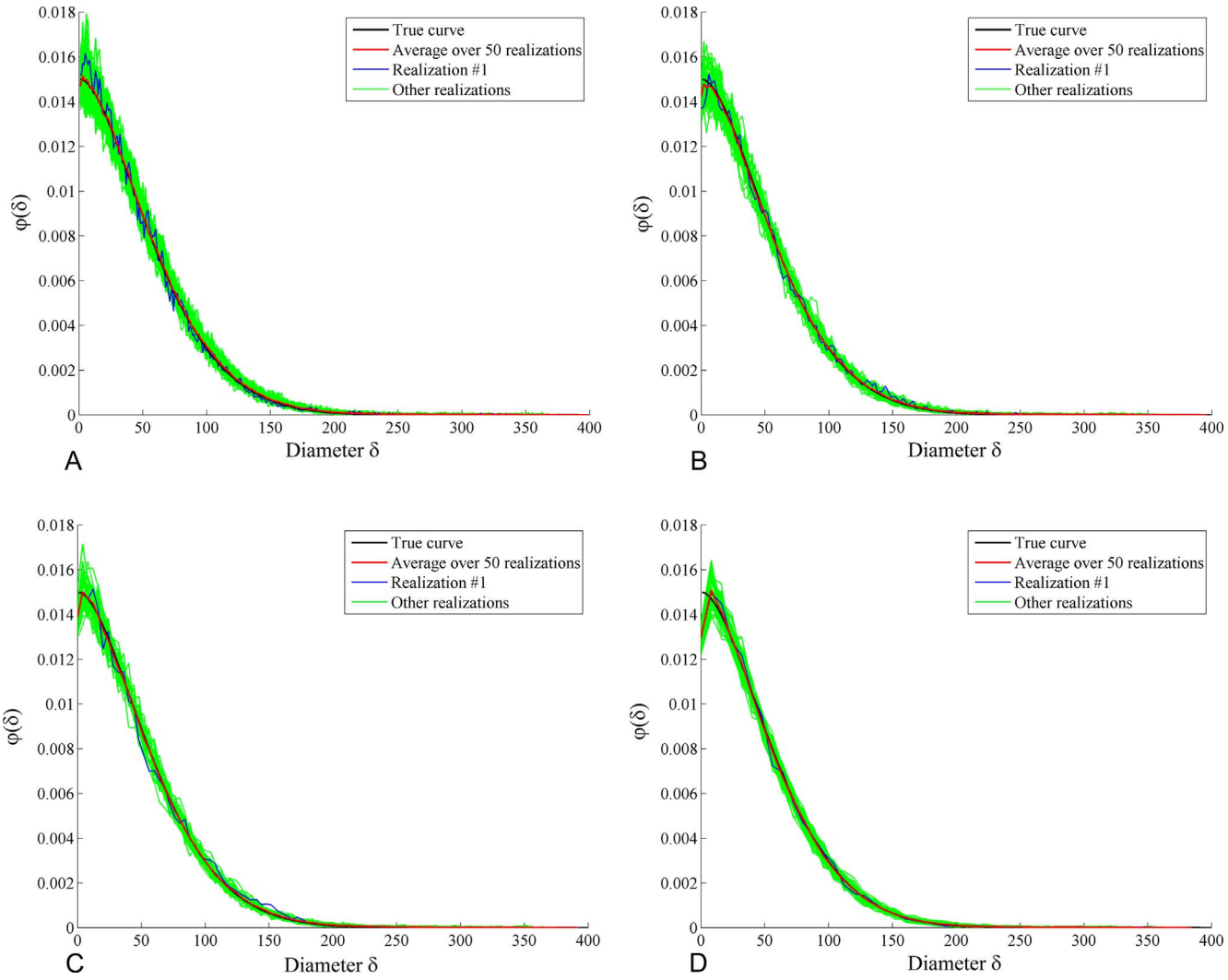

Fig. 4. Estimates of $\varphi(\delta)$ (blue and green), mean estimate (red) and true value (black) for experiments 3A, 3B, 3C and 3D.

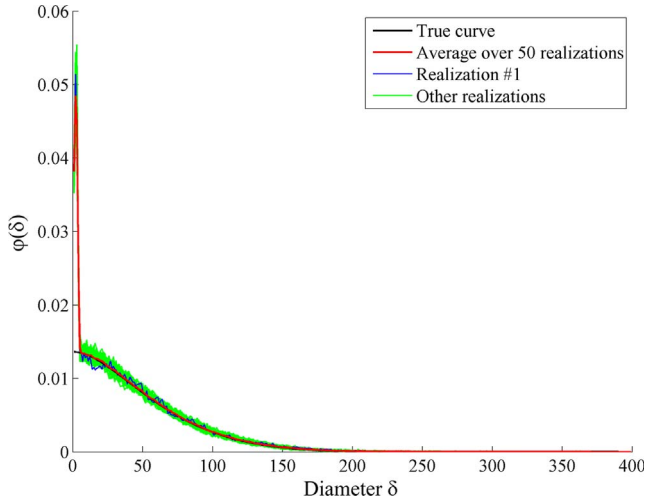

Fig. 5. Estimates of φ(δ) (blue and green), mean estimate (red) and true value (black) for experiment 4.

curve without bias, irrespective of the binning class width, although, as the latter increases, the resolution of the estimates decreases. In practice, when applying Eq. (19), there is no impediment to choose a small binning class width, so that the user can obtain the desired resolution for φ(δ).

4.5. Fourth experiment: Mixture of distributions

In the fourth experiment, the trace length sample is extracted from a mixture of two populations: the first one corresponds to the true trace length distribution and is associated with the same diameter distribution as in Experiment 1 C (a beta distribution with shape parameters $a = 2$ and $b = 10$ and a scale parameter $D_{max} = 400$), while the second population corresponds to noise, with a beta distribution with shape parameters $a = 5$ and $b = 5$ and a scale parameter 5. The numbers of observed trace lengths from these two distributions are set to $N_1 = 1000$ and $N_2 = 100$, respectively.

The estimates of φ(δ) are seen to fluctuate around the true fracture diameter distribution without bias for diameters greater than 5 (Fig. 5). Below this value, the curves deviate from the true one due to the presence of the noise distribution. Such a deviation complicates the estimation of the mean diameter μ_D of the underlying true distribution, since φ(0) and φ(1) are no longer representative of this distribution and their reciprocal are therefore biased estimates of μ_D. One solution is to estimate μ_D by 1/φ(5) in lieu of 1/φ(0), but this leads to a slight underestimation of φ(0) because φ(δ) is a non-increasing function, and thus a slight overestimation of μ_D. Another solution is to (i) replace the estimates of φ(0) to φ(4) by the estimate of φ(5) in order to remove the contribution of the noise, then (ii) consider the rescaled function φ(δ)/φ(0), which provides an estimate of the complementary cumulative distribution function $1 - G(\delta)$, and finally (iii) integrate this function, which directly yields an estimate of the mean value of the distribution. Indeed, the expectation of a nonnegative random variable is equal to the integral of its complementary cumulative distribution function [15]:

$$\mu_D = \int_0^{+\infty} [1-G(\delta)]\, d\delta \tag{22}$$

The estimates obtained with this last option prove to be more accurate than those obtained by considering 1/φ(0) or 1/φ(5) (Table 6).

5. Discussion and conclusions

The proposed approach (Eq. (19)) is distribution-free, insofar as it does not require choosing a parametric model for the trace length distribution or for the fracture diameter distribution. In this sense, it outperforms the forward modeling techniques, which must assume *a priori* that the fracture diameter distribution belongs to a certain family of distributions. Since the trace length distribution is moderately insensitive to large changes in the fracture diameter distribution, very different fracture diameter distributions can reasonably fit the observed trace length distribution, making the choice of the family of distributions a critical decision in all forward modeling techniques.

The proposed approach also outperforms the current inverse modeling techniques based on estimating, either analytically or numerically, the probability density function of the fracture diameters, which turns out to be an ill-posed problem. A substantial gain in robustness is obtained by estimating the cumulative distribution function instead of the density, allowing an unbiased estimation of this function. As observed in the numerical experiments, the dispersion of the estimation error decreases when the sample size increases (i.e., when more fracture trace lengths are observed) or when the diameter gets larger. Another benefit is the ability to estimate the mean and the higher-order moments (even for non-integer orders) of the fracture diameter distribution (Eqs. (20) and (21).

The proposed approach therefore appears as a simple and efficient alternative to estimate the fracture diameter distribution from an experimental estimate of the trace length distribution, requiring mild hypotheses. In addition to the assumptions of the Poisson-disc model, the only requirement to calculate Eqs. (18) to (21) is that the sample

Table 6
Estimates of mean diameter μ_D for fourth experiment.

Experiment	Estimator of μ_D	Minimum over P realizations	Maximum over P realizations	Average over P realizations	True value of μ_D
4	1/φ(0)	24.3	28.3	26.1	66.6
4	1/φ(5)	65.6	81.7	73.4	66.6
4	Integral of 1 – G(δ)	57.0	72.3	64.6	66.6

Table 7
Parameters for fifth experiment.

Experiment	Logarithmic mean	Logarithmic standard deviation	Mean fracture diameter	Number of realizations (P)	Number of fracture traces (N)	Truncation threshold δ_n	$1 - G(\delta_n)$
5A	4.605	0.333	105.7	50	1000	700	2.65×10^{-9}
5B	5.000	0.500	102.0	50	1000	1000	7.33×10^{-7}
5C	4.174	1.000	107.2	50	1000	2000	3.06×10^{-4}

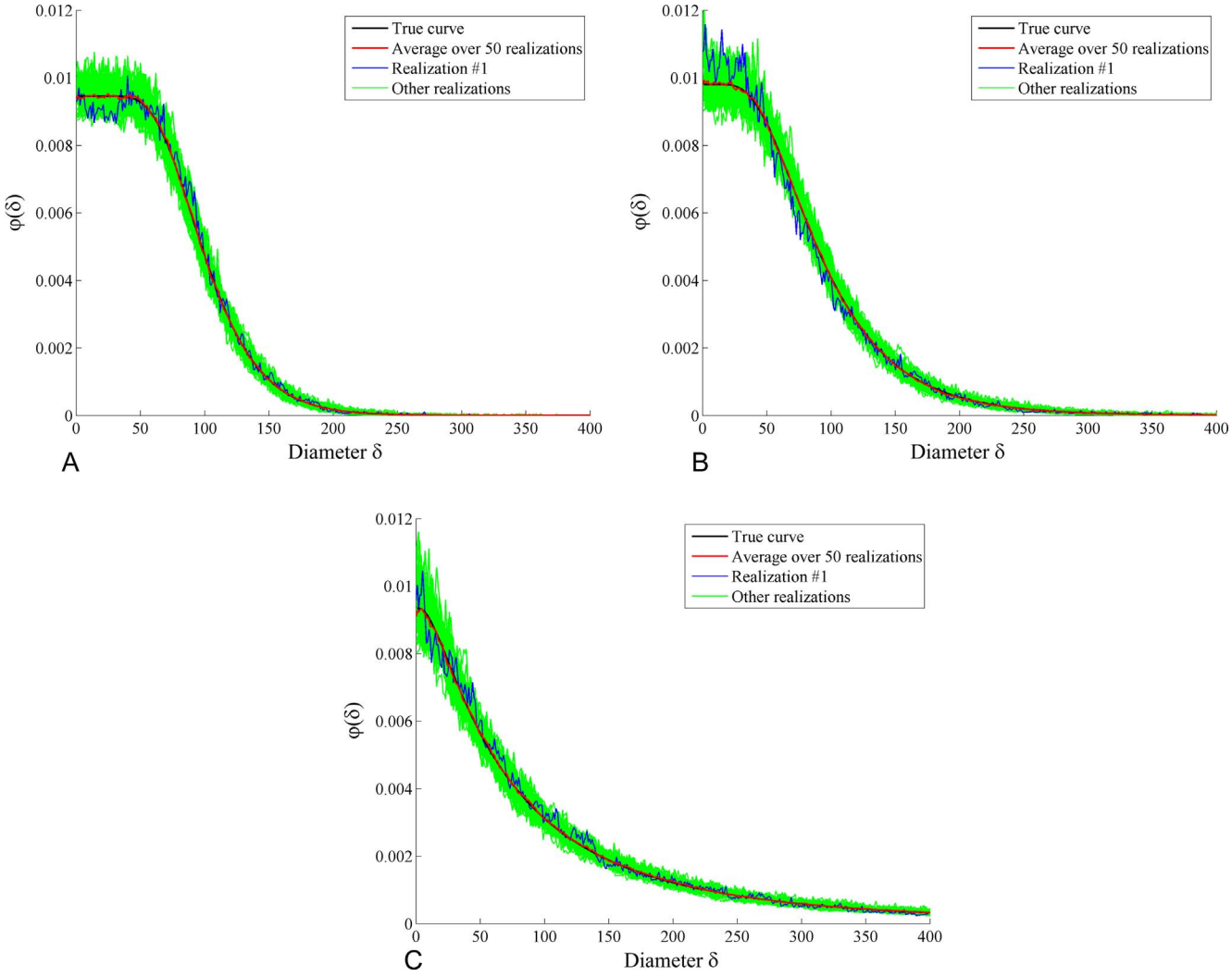

Fig. 6. Estimates of φ(δ) (blue and green), mean estimate (red) and true value (black) for experiments 5A, 5B and 5C.

trace length distribution has an upper bound, so that it has a discrete representation through a histogram $\hat{f}$ with a finite number of bins, which is always the case in practice (i.e., the sampled trace lengths always have a finite maximum value beyond which the trace length density can be assumed identically zero). As indicated in Section 2.1, the fracture diameter distribution needs not be absolutely continuous: even if this distribution is discrete or partially discrete, the trace length distribution will be absolutely continuous and possess a finite probability density function, except at the discontinuity points of G (*cdf* of the diameter distribution), and the proposed approach is therefore applicable.

Acknowledgements

This research was supported by the Chilean Commission for Scientific and Technological Research, through project CONICYT/FONDECYT/REGULAR/N°1170101.

Appendix A

Tonon and Chen [42] established the conditions that the trace length distribution should fulfill in order to provide a legitimate distribution for the fracture diameter:

(1) For all $\delta > 0$, $\frac{f(l)dl}{\sqrt{l^2-\delta^2}}$ is integrable on $[\delta, +\infty]$;
(2) $f(l)$ is positive in a positive neighborhood of zero;
(3) $f(l)$ decreases sufficiently fast as l tends to infinity.

Condition (1) is equivalent to stating that the integral in Eq. (8) is finite, i.e., the calculated complementary cumulative distribution function $1 - G(\delta)$ exists and is finite. Conditions (2) and (3) are needed to ensure that $G(\delta)$ is a non-decreasing function, from 0 when $\delta = 0$ to 1 when $\delta \to +\infty$.

However, the statement in condition (1) is incomplete, insofar as this condition should also be fulfilled for $\delta = 0$. For example Tonon and Chen [42] argue that a uniform trace length distribution between 0 and $b > 0$ provides a valid distribution for the fracture diameters. However, Eq. (8) gives the following complementary cumulative distribution function of the fracture diameters:

$$1-G(\delta)=\begin{cases}\frac{2\mu_D}{\pi b}\int_{\delta}^{b}\frac{dl}{\sqrt{l^2-\delta^2}} & \text{if } \delta < b\\ 0 & \text{otherwise}\end{cases} \tag{23}$$

For $\delta < b$, with the change of variable $l = \delta t$, one obtains:

$$1-G(\delta)=\frac{2\mu_D}{\pi b}\int_{1}^{b/\delta}\frac{dt}{\sqrt{t^2-1}}=\frac{2\mu_D}{\pi b}\ln\left(\frac{b}{\delta}+\sqrt{\left(\frac{b}{\delta}\right)^2-1}\right) \tag{24}$$

The right-hand side member of this equation tends to infinity as δ tends to zero, which is inconsistent with a genuine complementary cumulative distribution function. Accordingly, the uniform distribution is not a valid model for the trace length distribution.

Appendix B

In this appendix, we conduct an experiment (experiment 5) similar to the one described in Section 4.2 (experiment 1), but we replace the beta distribution for the fracture diameter by a lognormal distribution. In practice, since the latter distribution has an unbounded support, it is necessary to define an upper limit, i.e., to consider the distribution truncated to a finite interval $[0,\delta_n]$, in order to generate a sample of trace lengths and to subsequently apply Eqs. (19) to (21). Choosing an upper limit greater than the 99.9%-quantile of the true lognormal distribution yields results with no perceptible bias (Table 7 and Fig. 6).

References

[1] Aler J, Du Mouza J, Arnound M. Measurement of the fragmentation efficiency of rock mass blasting and its mining applications. Int J Rock Mech Min Sci Geomech Abstr 1996;33(2):125–40.
[2] Baecher GB, Lanney NA, Einstein HH. Statistical description of rock properties and sampling. Proc 18th US Symp Rock Mech Am Rock Mech Assoc. 1977. p. 1–8.
[3] Baecher GB, Lanney NA, 1978. Trace length biases in joint surveys. In: Proceedings of the 19th U.S. symposium on rock mechanics. Am Rock Mech Assoc, p. 56–65.
[4] Call RD, Savely JP, Nicholas DE, 1976. Estimation of joint set characteristics from surface mapping data. In: Proceedings of the 17th US symposium on rock mechanics. Am Rock Mech Assoc, p. 1–9.
[5] Chilès JP, Delfiner P. Geostatistics: modeling spatial uncertainty. New York: Wiley; 2012.
[6] Chilès JP, de Marsily G. Stochastic models of fracture systems and their use in flow and transport modeling. In: Bear J, Tsang CF, de Marsily G, editors. Flow and contaminant transport in fractured rocks. San Diego: Academic Press; 1993. p. 169–236.
[7] Cruden DM. Describing the size of discontinuities. Int J Rock Mech Min Sci Geomech Abstr 1977;14(3):133–7.
[8] Davis GH, Reynolds SJ. Structural geology of rocks and regions. New York: Wiley; 1996.
[9] Dershowitz W. Interpretation and synthesis of discrete fracture orientation, size, shape, spatial structure and hydrologic data by forward modeling. In: Cook NGW, Goodman RE, Myer LR, Tsang CF, editors. Fractured and jointed rock masses. Netherlands: Balkema; 1995. p. 579–86.
[10] Dershowitz WS, Herda HH. Interpretation of fracture spacing and intensity. In: Tillerson JR, Wawersik WR, editors. Rock Mechanics. Netherlands: Balkema; 1992. p. 757–66.
[11] Einstein HH, Baecher GB, Veneziano D, 1979. Risk analysis for rock slopes in open pit mines, Parts I-V. USBM Technical Report J0275015. Department of Civil Engineering, Massachusetts Institute of Technology.
[12] Emery X, Kracht W, Egaña A, Garrido F. Using two-point set statistics to estimate the diameter distribution in Boolean models with circular grains. Math Geosci 2012;44(7):805–22.
[13] Gorenflo R, Vessella S. Abel integral equations: analysis and applications. Berlin: Springer; 1991.
[14] Gradshteyn IS, Ryzhik IM. Tables of integrals, series, and products. New York: Academic Press; 2007.
[15] Grimmet G, Stirzaker D. Probability and random processes. Oxford: Oxford University Press; 2001.
[16] Hall P. Introduction to the theory of coverage processes. New York: Wiley; 1988.
[17] Hudson JA, Priest SD. Fracture and rock mass geometry. Int J Rock Mech Min Sci Geomech Abstr 1979;16(6):339–62.
[18] Jimenez-Rodriguez R, Sitar N. Inference of discontinuity trace length distributions using statistical graphical models. Int J Rock Mech Min Sci 2006;43(6):877–94.
[19] Kendall MG, Moran PAP. Geometrical probability. London: Charles Griffin and Co.; 1963.
[20] Kulatilake PHSW, Wathugala DN, Stephansson O. Joint network modeling with a validation exercise in Stripa Mine, Sweden. Int J Rock Mech Min Sci Geomech Abstr 1993;30(5):503–26.
[21] Kulatilake PHSW, Wu TH. Estimation of mean trace length of discontinuities. Rock Mech Rock Eng 1984;17(4):215–32.
[22] Kulatilake PHSW, Wu TH, 1986. Relation between discontinuity size and trace length. In: Proceedings of the 27th US symposium on rock mechanics. Am Rock Mech Assoc, p. 130–3.
[23] Lantuéjoul C. Geostatistical simulation: models and algorithms. Berlin: Springer; 2002.
[24] La Pointe PR, Wallmann PC, Dershowitz WS. Stochastic estimation of fracture size through simulated sampling. Int J Rock Mech Min Sci Geomech Abstr 1993;30(7):1611–7.
[25] Laslett GM. Censoring and edge effects in areal and line transect sampling of rock joint traces. Math Geol 1982;14(2):125–40.
[26] Loiseau P, 1988. Etude structurale et géostatistique des gneiss de la région du Cézallier (Massif Central Français): modélisation tridimensionnelle de réseaux de fractures, application à l'écoulement des fluides. PhD thesis, University of Orléans, Doc. BRGM no 162.
[27] Matheron G. Eléments pour une théorie des milieux poreux. Paris: Masson; 1967.
[28] Matheron G. Random sets and integral geometry. New York: Wiley; 1975.
[29] Mauldon M. Estimating mean fracture trace length and density from observations in convex windows. Rock Mech Rock Eng 1998;31(4):201–16.
[30] Pahl PJ. Estimating the mean length of discontinuity traces. Int J Rock Mech Min Sci Geomech Abstr 1981;18(3):221–8.
[31] Piteau DR, 1970. Geological factors significant to the stability of slopes cut in rock. In: Van Rensburg PWJ, editor. Proceedings of the symposium on the theoretical background to the planning of open pit mines with special references to slope stability. Balkema, Cape Town, p. 43–53.
[32] Priest SD. Discontinuity analysis for rock engineering. London: Chapman and Hall; 1993.
[33] Priest SD, Hudson JA. Estimation of discontinuity spacing and trace length using scanline surveys. Int J Rock Mech Min Sci Geomech Abstr 1981;18(3):183–97.
[34] Riley MS. Fracture trace length and number distributions from fracture mapping. J Geophys Res 2005;110:B08414.
[35] Robertson A. The interpretation of geologic factors for use in slope theory. In: Van Rensburg PWJ, editor. Proceedings of the symposium on the theoretical background to the planning of open pit mines with special references to slope stability. Balkema, Cape Town, 1970: p. 55–71.
[36] Santaló LA. Sobre la distribución de los tamaños de corpúsculos contenidos en un cuerpo a partir de la distribución en sus secciones o proyecciones. Trabajos de Estadística 1955;6(3):181–96.
[37] Santaló LA. Integral geometry and geometric probability. Addison-Wesley, Reading; 1976.
[38] Song JJ. Estimation of a joint diameter distribution by an implicit scheme and interpolation technique. Int J Rock Mech Min Sci 2006;43(4):512–9.
[39] Song JJ. Distribution-free method for estimating size distribution and volumetric frequency of rock joints. Int J Rock Mech Min Sci 2009;46(4):748–60.
[40] Song JJ, Lee CI. Estimation of joint length distribution using window sampling. Int J Rock Mech Min Sci 2001;38(4):519–28.
[41] Tonon F, Chen S. Closed-form and numerical solutions for the probability distribution function of fracture diameters. Int J Rock Mech Min Sci 2007;44(3):332–50.
[42] Tonon F, Chen S. On the existence, uniqueness and correctness of the fracture diameter distribution given the fracture trace length distribution. Math Geosci 2010;42(4):401–12.
[43] Villaescusa E, Brown ET. Maximum likelihood estimation of joint sizes from trace length measurements. Rock Mech Rock Eng 1992;25(2):67–87.
[44] Warburton PM. A stereological interpretation of joint trace data. Int J Rock Mech Min Sci Geomech Abstr 1980;17(4):181–90.
[45] Zhang L, Einstein HH. Estimating the intensity of rock discontinuities. Int J Rock Mech Min Sci 2000;37(5):819–37.
[46] Zhu H, Zuo Y, Li X, Deng J, Zhuang X. Estimation of the fracture diameter distributions using the maximum entropy principle. Int J Rock Mech Min Sci 2014;72:127–37.